

Switchable DNA-origami nanostructures that respond to their environment and their applications

Jasleen Kaur Daljit Singh, Minh Tri Luu, Ali Abbas, Shelley F. J. Wickham*

This is a post-peer-review, pre-copyedit version of an article published in Biophysical Reviews, October 2018, Volume 10, Issue 5, pp 1283–1293

The final authenticated version is available online at:

<https://doi.org/10.1007/s12551-018-0462-z>

1
2
3
4
5
6
7
8
9
10
11
12
13
14
15
16
17
18
19
20
21
22
23
24
25
26
27
28
29
30
31
32
33
34
35
36
37
38
39
40
41
42
43
44
45
46
47
48
49
50
51
52
53
54
55
56
57
58
59
60
61
62
63
64
65

Title:

Switchable DNA-origami nanostructures that respond to their environment, and their applications

Authors:

Jasleen Kaur Daljit Singh^{1,2,4}, Minh Tri Luu^{1,2,4}, Ali Abbas^{1,4}, Shelley F. J. Wickham^{*2,3,4}

1 School of Chemical and Biomolecular Engineering, The University of Sydney, Camperdown, New South Wales 2006, Australia.

2 School of Chemistry, University of Sydney, Camperdown, New South Wales 2006, Australia.

3 School of Physics, University of Sydney, Camperdown, New South Wales 2006, Australia.

4 University of Sydney Nano Institute, University of Sydney, Camperdown, New South Wales 2006, Australia.

* Corresponding author, shelley.wickham@sydney.edu.au

ORCID iD 0000-0002-5658-3546

Key words:

DNA origami, DNA nanotechnology, nanomachines, switchable nanostructures, actuation

Acknowledgments We thank Alice Williamson for helpful discussion and comments on the manuscript.

Author contributions S.W. and J.K.D.S. prepared figures, and wrote and edited the manuscript together, M.T.L. and A. A. contributed to manuscript editing and figures.

Compliance with ethical standards

Funding This work was supported by Australian Research Council Discovery Early Career Research Fellowship DE180101635 (SW), University of Sydney Nano Institute Scholarship (JKDS, MTL)

Conflict of interest Shelley Wickham declares that he has no conflict of interest. Jasleen Kaur Daljit Singh declares that she has no conflict of interest. Ali Abbas declares that he has no conflict of interest. Minh Tri Luu declares that he has no conflict of interest.

Ethical approval This article does not contain any studies with human participants or animals performed by any of the authors.

Abstract

1
2 Structural DNA nanotechnology, in which Watson-Crick base pairing drives the formation of self-
3 assembling nanostructures, has rapidly expanded in complexity and functionality since its inception
4 in 1981. DNA nanostructures can now be made in arbitrary 3-dimensional shapes and used to
5 scaffold many other functional molecules such as proteins, metallic nanoparticles, polymers,
6 fluorescent dyes and small molecules. In parallel, the field of dynamic DNA nanotechnology has
7 built DNA circuits, motors and switches. More recently, these two areas have begun to merge – to
8 produce switchable DNA nanostructures, which change state in response to their environment. In
9 this review, we summarize switchable DNA nanostructures into two major classes based on
10 response type: molecular actuation triggered by local chemical changes such as pH or
11 concentration, and external actuation driven by light, electric or magnetic fields. While molecular
12 actuation has been well explored, external actuation of DNA nanostructures is a relatively a new
13 area that allows for the remote control of nanoscale devices. We discuss recent applications for
14 DNA nanostructures where switching is used to perform specific functions - such as opening a
15 capsule to deliver a molecular payload to a target cell. We then discuss challenges and future
16 directions towards achieving synthetic nanomachines with complexity on the level of the protein
17 machinery in living cells.
18
19
20
21
22
23
24
25
26
27
28
29
30
31
32
33
34
35
36
37
38
39
40
41
42
43
44
45
46
47
48
49
50
51
52
53
54
55
56
57
58
59
60
61
62
63
64
65

Introduction

1 In biological systems, complex tasks are achieved by sophisticated molecular machines, such as
2 linear and rotary protein motors, ion pumps, and the DNA replication machinery (Alberts 1998). In
3 the emerging field of synthetic DNA nanotechnology (Seeman 1982), a range of nanoscale
4 machines and devices have been developed, that are both inspired by the protein machinery of the
5 cell and assembled from biomolecules. These DNA nanomachines have a range of potential
6 applications including: targeted drug delivery (Douglas et al. 2012; Perrault and Shih 2014; Li et al.
7 2018b), molecular computation (Zhang and Seelig 2011; Qian and Winfree 2011; Cherry and Qian
8 2018), in vitro diagnostics (Rinker et al. 2008; Godonoga et al. 2016), tools for biophysical
9 measurement of proteins (Rajendran et al. 2012; Derr et al. 2012; Iwaki et al. 2016; Omabegho et
10 al. 2018), templates for nano-electronic (Maune et al. 2010; Knudsen et al. 2015) or plasmonic
11 devices (Kuzyk et al. 2012; Gopinath et al. 2016; Lee et al. 2018), and even as molecular
12 assembly lines (Gu et al. 2010; Thubagere et al. 2017).

13
14
15
16
17
18
19
20
21
22 In structural DNA nanotechnology, base pairing drives the formation of self-assembling
23 nanostructures with arbitrary shapes (Seeman 1982). DNA is an ideal material for nanoscale
24 construction because DNA hybridisation is programmable, the rules of base-pairing are
25 predictable, and DNA is easily synthesised and chemically modified. 'DNA origami' is a robust
26 method for making custom DNA nanostructures in which a long single-stranded DNA 'scaffold'
27 strand is folded into a desired shape using shorter 'staple' strands (Rothemund 2006) (Figure 1).
28 DNA-origami nanostructures can be folded in 3-dimensions with complex curvature (Douglas et al.
29 2009; Dietz et al. 2009), and up to Gigadalton-scale (Wagenbauer et al. 2017). Functionalization of
30 DNA-origami nanostructures is achieved by covalent linkage of the guest molecule to a single-
31 stranded DNA (ssDNA) 'anti-handle', which hybridises to a complementary ssDNA 'handle' on the
32 surface of the DNA-origami nanostructure (Figure 1). Each staple strand has a unique nucleotide
33 sequence, so available handle sites on the DNA-origami nanostructure are uniquely addressable.
34 This allows for control of the number and geometry of functional molecules, with precision of ~ 6
35 nm (Rothemund 2006). DNA origami nanostructures have been used to scaffold many other
36 functional molecules such as nanoparticles (Lee et al. 2018), aptamers (Rinker et al. 2008;
37 Godonoga et al. 2016), proteins (Derr et al. 2012; Bell and Keyser 2016), fluorescent dyes (Yurke
38 et al. 2000) and small molecules (Zhao et al. 2012).

39
40
41
42
43
44
45
46
47
48
49
50
51
52 Switchable DNA nanostructures change from one state to another in response to changes in their
53 environment. This switch can be used to activate nanostructures to perform specific functions,
54 such as opening a capsule to deliver a molecular payload to a target cell (Douglas et al. 2012),
55 bringing proteins together to measure their interaction (Ke et al. 2016), or changing the chirality of
56 a plasmonic device (Kuzyk et al. 2014). Switching can be triggered by a local change in the
57 molecular environment. For example, addition of DNA oligonucleotides to trigger a strand
58
59
60
61
62
63
64
65

1 displacement reaction (Yurke et al. 2000; Andersen et al. 2009; Song et al. 2017; Thubagere et al.
2 2017), change in pH (Surana et al. 2011; Burns et al. 2018) or ionic concentration (Mao et al.
3 1999; Sannohe et al. 2010; Gerling et al. 2015), or addition of proteins (Douglas et al. 2012;
4 Godonoga et al. 2016; Li et al. 2018b) or other small molecules (Zadegan et al. 2017). Recently,
5 progress has been made towards achieving switchable DNA nanostructures that respond to
6 external changes, such as light (Derr et al. 2012; Kuzyk et al. 2016; Willner et al. 2017; Liu et al.
7 2018a), and electric (Kroener et al. 2017; Kopperger et al. 2018) or magnetic fields (Lauback et al.
8 2018). External actuation has the potential to provide remote control of nanostructures,
9 independent of their chemical environment, inside cells or tissue. In this review, we give an
10 overview of both molecular and external actuation methods used to switch DNA-origami
11 nanostructures, and their potential applications. We also discuss future directions in this field, and
12 fundamental limits and challenges towards *in vivo* implementation.
13
14
15
16
17
18
19
20
21
22

23 **Molecular Actuation of DNA-origami nanostructures**

24 *DNA Strand displacement*

25
26
27 If a DNA strand is hybridised to a shorter strand, an overhanging 'toe-hold' will remain as ssDNA.
28 When a fully complementary DNA strand is added, this will bind to the toe-hold, and displace the
29 shorter strand – in a process known as toe-hold mediated DNA strand displacement (Figure 2).
30 The first switchable DNA device triggered by strand displacement was a DNA tweezer, assembled
31 from 3 DNA strands, that opens or closes on manual addition of DNA 'fuel' or 'anti-fuel' strands
32 (Yurke et al. 2000). Similarly, the first switchable DNA-origami nanostructure, a 3-dimensional
33 DNA-origami box, was opened by strand displacement (Andersen et al. 2009). DNA strand
34 displacement has been used to implement a variety of molecular systems, including autonomous
35 DNA motors that navigate complex tracks (Wickham et al. 2012; Thubagere et al. 2017; Li et al.
36 2018a), DNA-origami switches (Marini et al. 2011; Torelli et al. 2014; Zhou et al. 2015), and to
37 create complex logic circuits such as a DNA-based winner-take-all neural network for molecular
38 pattern recognition (Cherry and Qian 2018). DNA strand displacement reactions are a powerful
39 method for sophisticated actuation, and can accommodate many different molecular triggers in
40 parallel. However, they require DNA fuel strands as input and generate waste.
41
42
43
44
45
46
47
48
49
50
51
52

53 *Ionic concentration*

54 One of the earliest nanomechanical DNA devices was driven by changing ionic concentration (Mao
55 et al. 1999). High salt concentrations and low temperature can cause dsDNA with the sequence
56 (CG)_n to be switched from the usual right-handed helix (B-DNA) to a left-handed conformation (Z-
57 DNA), and this change in twist was used to drive rotary motion. The fundamental 4-way (Holliday)
58
59
60
61
62
63
64
65

1 junction that forms the basis of DNA nanotechnology is also sensitive to divalent cation
2 concentration, adopting an open square planar geometry in the absence of cations, and a stacked
3 X-shaped structure, with an angle of $\sim 60^\circ$, above ~ 0.1 mM MgCl_2 (Lilley 2000). However, DNA-
4 origami nanostructures are not generally stable below ~ 2 mM MgCl_2 , so this is not a generalisable
5 switching strategy (Hahn et al. 2014). Blunt end stacking of DNA helices can be used for hierarchal
6 assembly of DNA-origami nanostructures into larger 'crystals', based on shape-complementarity
7 (Gerling et al. 2015). This stacking interaction is sensitive to the concentration of counter ions in
8 solution because of the repulsion between the negatively charged surfaces of the DNA-origami.
9 This effect has been used to create both discrete DNA-origami nanostructures and extended DNA-
10 origami lattices that change shape in response to change in magnesium concentration. Similarly,
11 rearrangement of DNA stacking interactions can be exploited to propagate information transfer
12 across a DNA-origami nanostructure, and has been directly observed by Atomic Force Microscopy
13 (AFM) (Song et al. 2017). Alternatively, G-quadruplexes are built from the stacking of successive
14 G-tetrads, which are cyclic Hoogsteen bonded square planar alignments of four guanines that are
15 stabilized by bound monovalent Na^+ and K^+ cations (Figure 3) (Patel et al. 2007). Two guanine-
16 rich strands can be incorporated into the DNA nanostructure, which form an interstrand G-
17 quadruplex structure in the presence of K^+ and disassemble on removal of K^+ , which can be used
18 to trigger switching (Figure 2) (Sannohe et al. 2010; Kuzuya et al. 2011).

30 *Protein and aptamer actuation*

31 Another molecular method for DNA-origami actuation is through interaction with proteins.
32 DNA modifying proteins, as such as restriction enzymes, can be used for site-specific cleavage of
33 the DNA backbone on one side of the double helix. Once cleaved, small DNA fragments ($< \sim 5$
34 nucleotides) will dissociate, revealing a ssDNA toe-hold which is then available for strand
35 displacement. This method has been used to power a number of DNA motors and machines
36 (Figure 2) (Bath and Turberfield 2007; Wickham et al. 2012). Binding of DNA aptamers to protein
37 ligands has also been used for actuation (Rinker et al. 2008; Kuzuya et al. 2011; Douglas et al.
38 2012; Godonoga et al. 2016; Li et al. 2018b). Aptamers are DNA oligonucleotides that bind specific
39 molecular targets (Hamaguchi et al. 2001), and can be used in systems where a complementary
40 DNA strand forms a duplex with the aptamer. Binding of the target molecule destabilises the
41 duplex state, dissociating the aptamer strand from the complementary DNA strand, inducing
42 switching of the DNA-origami structure (Figure 2). For example, aptamer switching has been used
43 to release drug payloads on binding to specific cell surface receptors (Douglas et al. 2012; Li et al.
44 2018b). The use of targeting ligands to drive switching allows the DNA-origami nanostructures to
45 act autonomously, without external intervention, but does not generally allow for mechanisms that
46 are reversible, unless coupled with DNA strand displacement (Kuzuya et al. 2011).

60 *Change in pH*

1 pH sensors are of particular interest as components of switchable DNA-origami nanostructures for
2 *in vivo* applications, because acidic conditions are found in the endosomal pathway after cell entry,
3 and in cancer tissue (Gerweck and Seetharaman 1996). There are two common pH switches used
4 in DNA nanotechnology (Figure 2). The first is the i-motif: a quadruplex structure formed from a
5 cytosine rich ssDNA at an acidic pH (Gehring et al. 1993). This structure consists of intercalated
6 semiprotonated C·C⁺ base pairs, and requires protonation of cytosine at the N3 position (with a
7 pKa below 7), and thus is triggered by change in pH (Figure 3). The second is a DNA triplex,
8 formed by pH-sensitive sequence-specific parallel Hoogsteen bonding between a dsDNA strand
9 and a ssDNA strand (Figure 3) (Frank-Kamenetskii and Mirkin 1995). These triplexes contain CGC
10 pairings that are only stabilized at acidic pH because they require protonation of the ssDNA
11 cytosine at N3 position pH (pKa ≈ 6.5), and TAT pairings that only destabilize at alkaline pH due to
12 the deprotonation of thymine (pKa ≈ 10). The pH sensitivity of the DNA triplex can be controlled by
13 tuning its CGC/TAT content (Idili et al. 2014). Both i-motifs and triplex DNA switches are
14 convenient because their behaviour is predictable and can be tuned to a narrow range of pH
15 changes.
16
17
18
19
20
21
22
23
24

25 I-motifs have been used for pH switching of several DNA-origami nanostructures. Kuzuya et. al.
26 developed DNA-origami pliers: a 170 nm lever structure decorated with cytosine rich ssDNAs that
27 form i-motifs at acidic pH (Kuzuya et al. 2014). At slightly alkaline or neutral pH, the pliers take
28 either a cross or antiparallel position, where the ssDNAs are exposed. In slightly acidic conditions
29 (pH 5.6), the i-motifs form and lock the arms in place, resulting a parallel structure. Similarly,
30 Majikes et. al. used i-motifs to control the distance between two DNA-origami substructures, with
31 reversible switching (Majikes et al. 2017). More recently, Burns et. al. demonstrated protein
32 delivery to cells using a pH switchable DNA-origami box with a lid controlled by i-motifs (Burns et
33 al. 2018). Upon entering the cell, the box encounters the acidic conditions of the endosome,
34 opening the lid and releasing green fluorescent proteins (GFP) from inside the box.
35
36
37
38
39
40
41
42
43

44 DNA triplex locks have been used for pH actuation of a number of DNA-origami nanostructures,
45 including a cross-like plasmonic DNA nanostructure decorated with two gold nanorods (Kuzyk et
46 al. 2017). At low pH (<6.5), a duplex on one arm of the cross DNA binds to a ssDNA on the other
47 arm, to form a DNA triplex, locking the origami structure. As the pH is increased, the triplex is
48 unlocked and the origami returns to the relaxed state. A left or right-handed nanoparticle
49 confirmation can be achieved by manipulating the location of the triplex lock, and pH sensitivity is
50 tuned by changing the TAT content of the lock strand.
51
52
53
54
55
56

57 A pH-actuated version of the original DNA tweezer has been successfully applied as an *in vivo* pH
58 sensor. Surana et. al. show that an i-motif based DNA nanomachine coupled with fluorescence
59 resonance energy transfer (FRET) measurements could be used to effectively map spatiotemporal
60
61
62
63
64
65

pH changes associated with endosomal maturation in different types of *Caenorhabditis elegans*. This was the first successful employment and actuation of a DNA nanomachine in an organism (Surana et al. 2011). In subsequent work, a pH responsive I-switch was developed for specific organelles in the cell, such as the trans Golgi network (TGN), cis Golgi (CG) and endoplasmic reticulum (ER), which all have different pH. This allowed for simultaneously live-cell tracking of pH in two different organelles (Modi et al. 2013). An interesting extension of this would be to couple pH measurement to pH-responsive drug delivery to specific organelles.

External actuation of DNA-origami nanostructures

Photoactuation

Three techniques are used for photoactuation in DNA nanotechnology: photoswitching, photocleavage and photocaging. The most common method is the photoswitching of azobenzene attached to the DNA backbone (Figure 3). Asanuma et. al. show that the formation of an azobenzene-modified DNA duplex can be photo-regulated using ultraviolet (UV) and visible light (Asanuma et al. 2007). Azobenzene takes a cis-form when exposed to UV light (300-400nm), which inhibits DNA hybridisation. In contrast, the azobenzene takes a trans-form when exposed to visible light (>400nm), which allows formation of a stable DNA duplex. Photocleavage is achieved by incorporating a photocleavable (PC) linker into the DNA backbone. The linker is cleaved when exposed to UV light, thereby breaking the DNA strand. Photocleavage of oligonucleotides has been demonstrated with several chemical modifications, including o-nitrobenzyl ethers (Ordoukhanian and Taylor 1995), 2-nitrobenzyl (Bai et al. 2003; Li et al. 2003) and 7-diethylaminocoumarin (Weyel et al. 2017). Photocaging refers to the act of 'caging' active molecules with a photolabile group, thereby preventing activity of the molecule. Upon exposure to light of the correct wavelength, the molecule is freed of the 'cage' and is active again. Photocaged DNA strands have been used for the photoregulation of DNA function (Liu and Deiters 2014), DNA aptamer activation (Heckel and Mayer 2005), DNAzyme activation (Hwang et al. 2014), and for DNA computation using logic gates (Prokup et al. 2012).

Both photoswitching and photocleavage have been used for DNA-origami nanostructure actuation. Yang et. al. developed photoresponsive DNA-origami hexagons by connecting them to azobenzene-modified oligonucleotides (Azo-ODNs) (Yang et al. 2012). By manipulating the number and positions of the Azo-ODNs on the origami units, different origami hexagons could be linked together via photo-actuation of the Azo-ODNs to form larger 2-dimensional structures of different shapes. Azo-ODNs have also been used to form photoswitchable DNA origami nanocapsules (Takenaka et al. 2014), that open when exposed to UV light and close when exposed to visible light. More recently, reversible photo-actuation of cross-shaped DNA-origami

1 nanostructures was achieved by photoisomerization of azobenzene modifications in a 'lock' duplex
2 (Kuzyk et al. 2016; Willner et al. 2017). When exposed to UV light, the azobenzenes transform to
3 cis-form, resulting in dehybridization of the lock strands and opening of the structure. However, the
4 reversibility of azobenzene-modified DNA is temperature sensitive (Samai et al. 2017), and
5 reversible switching requires a high number of modifications – in these examples, 7 modifications
6 in a 10 or 20 base-pair duplex (Kuzyk et al. 2016; Willner et al. 2017).
7
8
9

10 Photocleavable linkers have been used for payload release from DNA origami nanostructures
11 (Kohman et al. 2016). In this example, proteins were loaded onto a rectangular DNA-origami
12 structure via a o-nitrobenzyl based PC linker and an alkyne oligo. Upon exposure to UV light, the
13 PC linker was cleaved resulting in the release of the protein. Similarly, the linear protein motors
14 dynein and kinesin, which move in opposite directions along microtubules, have been conjugated
15 to a DNA-origami 'chassis' by PC linkers (Derr et al. 2012). UV light was used to cleave the PC
16 linkers, giving selective detachment of one type of motor protein, which controlled the subsequent
17 direction of the DNA-origami chassis along the microtubule. While photocaging has not been used
18 for DNA-origami nanostructures actuation, it recently been used for actuation of a simple DNA
19 tweezer (Liu et al. 2018a). While irreversible, this actuation was measured to be ~ 60 times faster
20 than strand displacement, and simulations predicted that forces of up to 46 pN were generated.
21
22
23
24
25
26
27
28
29

30 Overall, photoactuation is a simple, fast and effective method for structural switching. Currently,
31 photocleavage and photocaging do not allow for reversible actuation, while photoswitching only
32 has limited reversibility. Another limitation of photoactuation is that it relies on UV radiation, which
33 damages DNA, most commonly through formation of cyclobutane pyrimidine dimers (CPDs)
34 between neighbouring pyrimidines residues (Vink and Roza 2001). UV damage of DNA is
35 wavelength dependent and is particularly dominant at UVB (280–315 nm) and UVC (200–280 nm)
36 wavelengths. Chen et. al. (Chen et al. 2017) showed that UVB and UVC cause a 'flattening' effect
37 in DNA-origami nanostructures, as the UV radiation relieves internal stress in the origami. At high
38 UV doses, the DNA-origami nanostructures are damaged. UVA (315– 400 nm), on the other hand,
39 showed no conformational damage to the DNA-origami nanostructures. Another limitation of UV
40 radiation is that it has low penetration depth (< 1 mm) and therefore is less useful for the
41 photoactuation of DNA-origami nanostructures *in vivo* (Anderson and Parrish 1981).
42
43
44
45
46
47
48
49
50
51

52 *Electrical actuation*

53 The phosphate backbone of DNA results in DNA-origami nanostructures that have a net negative
54 charge. Thus, electric fields can be used to actuate them. Kroener et. al. demonstrated electrical
55 switching of a 100-nm long DNA-origami nanolever on a gold electrode (Kroener et al. 2017).
56 Fluorescence intensity was used to measure the angle between the lever and the electrode, as the
57 surface acts to quench fluorescence (Chance et al. 2007). An alternating low frequency voltage of
58
59
60
61
62
63
64
65

1
2
3
4
5
6
7
8
9
10
11
12
13
14
15
16
17
18
19
20
21
22
23
24
25
26
27
28
29
30
31
32
33
34
35
36
37
38
39
40
41
42
43
44
45
46
47
48
49
50
51
52
53
54
55
56
57
58
59
60
61
62
63
64
65

± 200 mV was applied. At negative potentials, the negatively charged levers were repelled into a standing position, while at positive potentials they were attracted to the surface, with a response time of less than 100 μ s.

In more recent work, Kopperger et. al. demonstrated the electrical actuation of a flexible DNA-origami arm on a DNA-origami platform (Kopperger et al. 2018) (Figure 4). The platform was decorated with multiple ssDNA 'latches', complementary to a ssDNA 'catch' on the arm. The catch on the arm hybridizes to a complementary latch on the base platform at a position that is determined by the direction of the external electric field. As the applied electric field is rotated, the arm moves from one position to another in less than a millisecond. The arm can also be used to transport gold nanorods from one side of the platform to the other. In the future, this could be coupled to cargo-transfer mechanisms (Kassem et al. 2016; Thubagere et al. 2017) to result in computer directed arrangement of molecules using DNA origami. A challenge in applying electrical switching *in vivo* is that the electric field can cause heating and damage, and must be kept below 30–40 kV/m (Menachery and Pethig 2005).

Magnetic actuation

While DNA-origami nanostructures are not intrinsically magnetic, they can be functionalised with magnetic nanoparticles. Generally, to actuate a DNA-origami nanostructures require a force and torque of ~ 1 pN and 10–50 pN·nm, respectively (Marras et al. 2015). However, to achieve forces of this magnitude with a magnetic field requires superparamagnetic beads of 1 μ m or larger (Xu et al. 2016). In a recent advance, Lauback et. al. bridged this difference in scale by using a highly stiff microscale lever as the link between a microscale magnetic nanoparticle and a nanoscale DNA-origami device (Lauback et al. 2018) (Figure 4). The system consists of 3 components: a lever, a rotor and a hinge, all constructed from 56-helix DNA-origami nanobricks. The lever was designed to be both mechanically stiff, and long enough (1 μ m) for coupling to a micron scale magnetic nanoparticle. The other end of the lever was fixed to the surface, and an externally applied magnetic field was used to drive rotation of the bead and in turn, of the lever. The lever was connected to the platform by either a DNA-origami rotor, to achieve continuous rotational motion, or a DNA-origami hinge, to achieve finite angular motion. Rotational motion was controlled to a frequency of 2 Hz with up to 80 pN·nm of torque, while the angular motion was specified with accuracy of $\pm 8^\circ$.

Discussion

An ideal actuation method for a nanomachine would be fast, reversible, able to process many inputs independently, produce both digital and analogue responses, allow both local and external control, and not generate waste heat or by-products. While a range of methods have been used to

1
2
3
4
5
6
7
8
9
10
11
12
13
14
15
16
17
18
19
20
21
22
23
24
25
26
27
28
29
30
31
32
33
34
35
36
37
38
39
40
41
42
43
44
45
46
47
48
49
50
51
52
53
54
55
56
57
58
59
60
61
62
63
64
65

actuate DNA-origami nanostructures that cover this range of properties, as yet no single method is able to provide all. Currently, the specific choice of method depends on the application.

DNA strand displacement is still the best method for multiplexing many trigger molecules in parallel, and is reversible, but requires external DNA strand input and generates waste. In comparison, both aptamer and pH actuation allow for autonomous switching in *in vivo* settings, as no external interaction is required after delivery into an organism. However, these methods currently lack reversibility and their response cannot be modified externally after delivery. In the future, the ability to link multiple pH or aptamer switches together to produce DNA-origami nanostructures that are activated in response to a more complex set of environmental triggers would increase the utility of these methods. For example, by incorporating multiple i-motifs that are each tuned to a different pH into the same DNA-origami nanostructure so that it is activated only within a certain pH window, and can reversibly switch off at either higher or lower pH. Another example would be an aptamer actuated DNA nanocapsule that is only activated after processing a complex set of local conditions, such as up-regulation of one set of cell-surface receptors above a certain threshold, and down-regulation of another set.

For applications that require greater control of DNA-origami nanostructures, the use of external actuation that can be more easily controlled at the macroscale (such as light, electric and magnetic field) shows great potential. Among these, light-based switching of DNA-origami nanostructures is the most well-developed. A limitation of current photoactuation methods is the use of wavelengths that damage cells (UV), and do not penetrate tissue (UV-Vis). The development of photoswitching systems that utilise tissue-penetrating photons, that typically exists in the near infrared (NIR) wavelength range of 630–950nm, would increase the utility of this approach (Weissleder 2001; Frangioni 2003). For example, if recently developed NIR photoswitching molecules (Yang et al. 2014) were conjugated to DNA, it may allow photoswitching of DNA-origami nanostructures *in vivo*. Another promising future direction is DNA-origami nanostructures that can be driven through a multi-state switching cycle by sequential activation at a number of different wavelengths. To achieve this requires development of a range of photoswitching molecules that can be spectrally multiplexed.

While photoactuation is currently useful for applications that require digital switching of DNA-origami nanostructures between discrete states, electrical or magnetic switching can be more appropriate for analogue switching through a range of states. The use of applied electric and magnetic fields also allows for reversibility, does not generate waste and results in a fast response time. Sub-second response times have been demonstrated with current electrical and magnetic switching *in-vitro*. Electrical switching does not require the attachment of DNA-origami nanostructures to a 'switching molecule' as the DNA-origami nanostructure itself is negatively

1 charged. Magnetic switching on the other hand requires the attachment of the DNA-origami
2 nanostructure to a superparamagnetic bead.

3
4 In our view, recent advances in using electric and magnetic fields to switch DNA-origami
5 nanostructures will promote rapid development of these structures for use *in vivo*. While this area
6 has much potential, more generally, there are some fundamental limits to the application of
7 switchable DNA-origami nanostructures. *In vivo* applications are limited by biostability and
8 biocompatibility. The structural integrity of DNA-origami nanostructures is compromised in
9 physiological fluids due to nuclease degradation and low levels of salt (Hahn et al. 2014).
10 Promisingly, the stabilization of DNA-origami nanostructure has been demonstrated using lipid-
11 wrapping (Perrault and Shih 2014) and coating with an oligolysine-polyethylene (PEG) shell
12 (Ponnuswamy et al. 2017). DNA-origami nanostructures are also sensitive to both mechanical and
13 thermal damage. The force required to melt DNA is in the pN region (Santosh and Maiti 2009) and
14 so is the force needed for the rupture of DNA-origami nanostructures (Engel et al. 2018). This
15 limits the external force that can be placed on these systems by electric and magnetic fields. In
16 comparison, the force required to rupture liposomes is 3 orders of magnitude larger (nN) (Wang et
17 al. 2012). Similarly, external fields applied should be low enough in power that bulk heating of the
18 solution does not melt the DNA-origami nanostructures, which begins at approximately 40 °C, or
19 damage cells, which for electric fields occurs above 30–40 kV/m (Menachery and Pethig 2005). UV
20 cross-linking agents can be used to increase thermal stability of DNA-origami nanostructures up to
21 85 °C (Rajendran et al. 2011), but does not protect the surrounding tissue.

22
23 Overall, switchable DNA-origami nanostructures have been used to construct functional
24 nanomachines that can respond to either their local chemical environment or be remotely
25 controlled. However, the complexity of these synthetic devices and their applications is still far
26 below that of even the simplest protein machinery found in living cells. To achieve the goal of
27 functional nanomachines will require both the development of new actuation methods and the
28 enhancement of existing methods. The combination of multiple methods across scales also has
29 the potential to rapidly increase the complexity and utility of these devices. For example, for *in vivo*
30 applications magnetic switching could be used to trigger drug delivery at a target site on the
31 macroscale, coupled with pH-gated activation at the cellular level. Development of new multiscale
32 frameworks to represent, design and program such systems will facilitate this. Rapid advances in
33 high spatial and time-resolution molecular imaging (Schueder et al. 2017; Liu et al. 2018b) will also
34 drive the development of complex DNA machinery, by allowing direct observation of the dynamics
35 of nanostructures actuation both *in vitro* and *in vivo*. The ultimate goal of this would be to make
36 real-time observations of complex DNA-origami nanodevices changing shape at the single-
37 molecule level in live organisms.

1
2
3
4
5
6
7
8
9
10
11
12
13
14
15
16
17
18
19
20
21
22
23
24
25
26
27
28
29
30
31
32
33
34
35
36
37
38
39
40
41
42
43
44
45
46
47
48
49
50
51
52
53
54
55
56
57
58
59
60
61
62
63
64
65

1
2
3
4
5
6
7
8
9
10
11
12
13
14
15
16
17
18
19
20
21
22
23
24
25
26
27
28
29
30
31
32
33
34
35
36
37
38
39
40
41
42
43
44
45
46
47
48
49
50
51
52
53
54
55
56
57
58
59
60
61
62
63
64
65

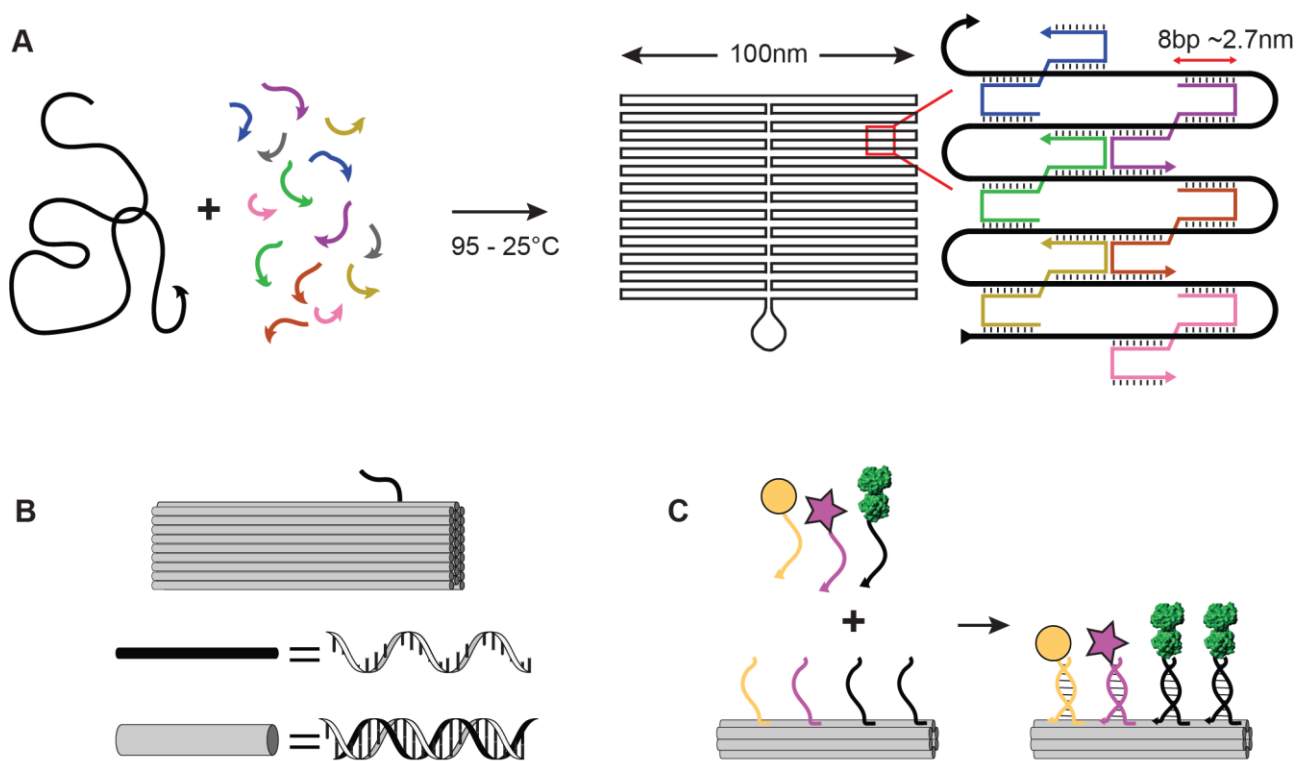


Fig. 1 DNA-origami nanostructures. **a** In DNA Origami, a long single-stranded DNA scaffold (black) is folded up into a double-stranded DNA shape, which is cross-linked by ~300 short 'staple' oligonucleotide strands (coloured). **b** DNA-origami nanostructures are often depicted by representing each DNA duplex with a rigid cylinder of width 2.6 nm (grey), and single-stranded DNA regions with a flexible line (black). **c** DNA-origami nanostructures can be functionalised by adding single-stranded DNA 'handles' to the 3' end of staple strands on the surface of the structure (coloured). Each staple sequence is unique, so handle locations are uniquely addressable. Guest molecules, such as metallic nanoparticles (yellow), fluorophores (pink) or proteins (green), are covalently linked to complementary 'anti-handle' sequences. On incubation with the DNA-origami nanostructure, guest molecules are scaffolded by the origami with precision of up to ~ 6 nm.

1
2
3
4
5
6
7
8
9
10
11
12
13
14
15
16
17
18
19
20
21
22
23
24
25
26
27
28
29
30
31
32
33
34
35
36
37
38
39
40
41
42
43
44
45
46
47
48
49
50
51
52
53
54
55
56
57
58
59
60
61
62
63
64
65

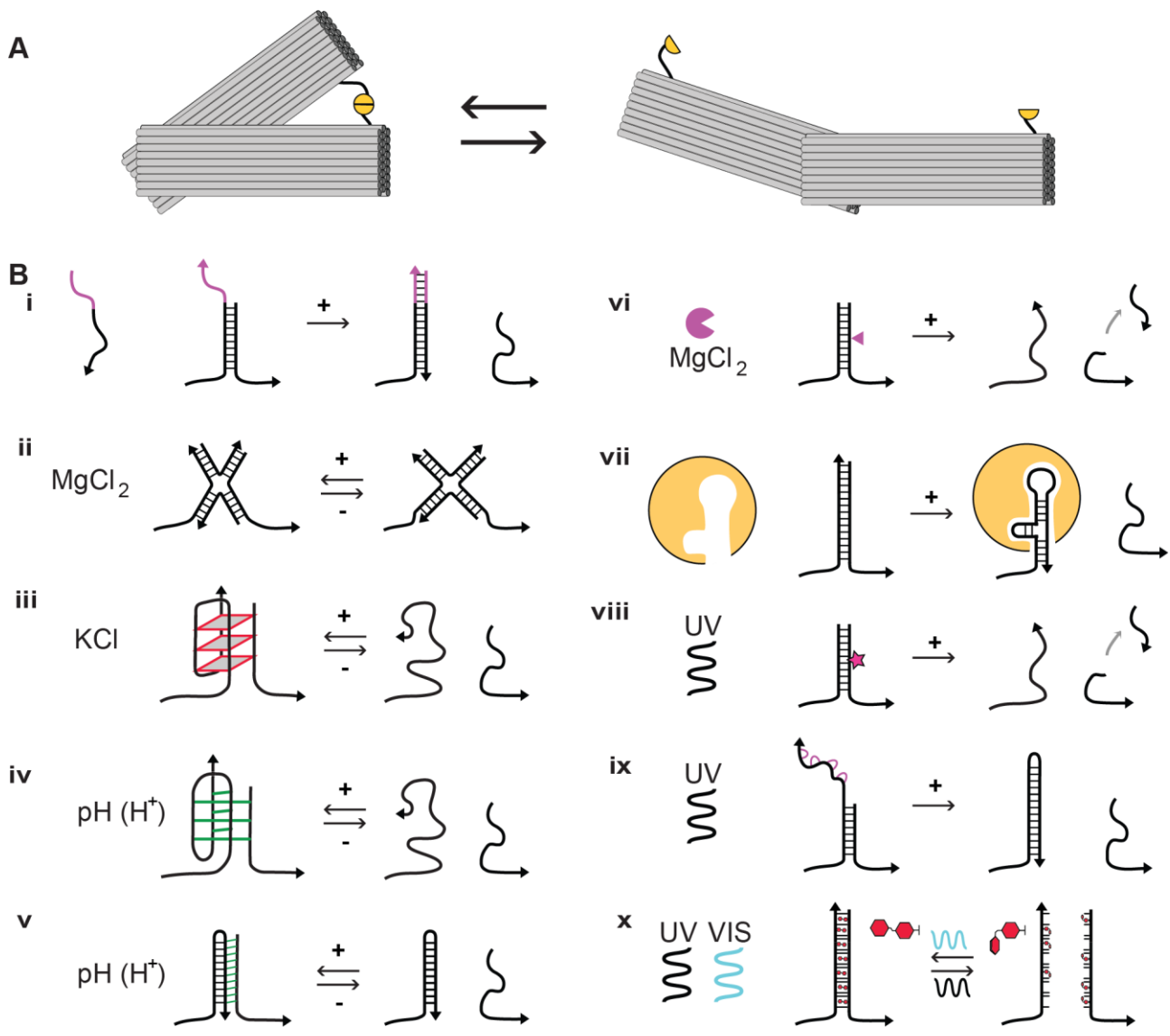


Fig. 2 Switchable DNA-origami nanostructures actuated by local molecular signals and externally by light. **a** DNA-origami nanostructures can be designed with flexible regions, and a number of possible states. For example, a DNA-origami tweezer, or caliper, can be either closed (left) or open (right), depending on the state of a molecular 'lock' that links the two arms (yellow). **b** A range of methods can be used to open the lock, actuating the DNA-origami nanostructure. **i** DNA strand displacement reaction on addition of ssDNA 'trigger', **ii** stacking interaction change on addition of $MgCl_2$, **iii** G-quadruplex formation on addition of KCl, **iv** i-motif formation on decrease in pH, **v** DNA triplex formation on decrease in pH, **vi** enzymatic cleavage of DNA backbone, **vii** ligand-stabilisation of DNA aptamer structure, **viii** photo-cleavage of modified DNA backbone with UV light, **ix** release of photo-caged based by UV light, **x** reversible photo-switching of azobenzene modified DNA bases by UV and Visible light.

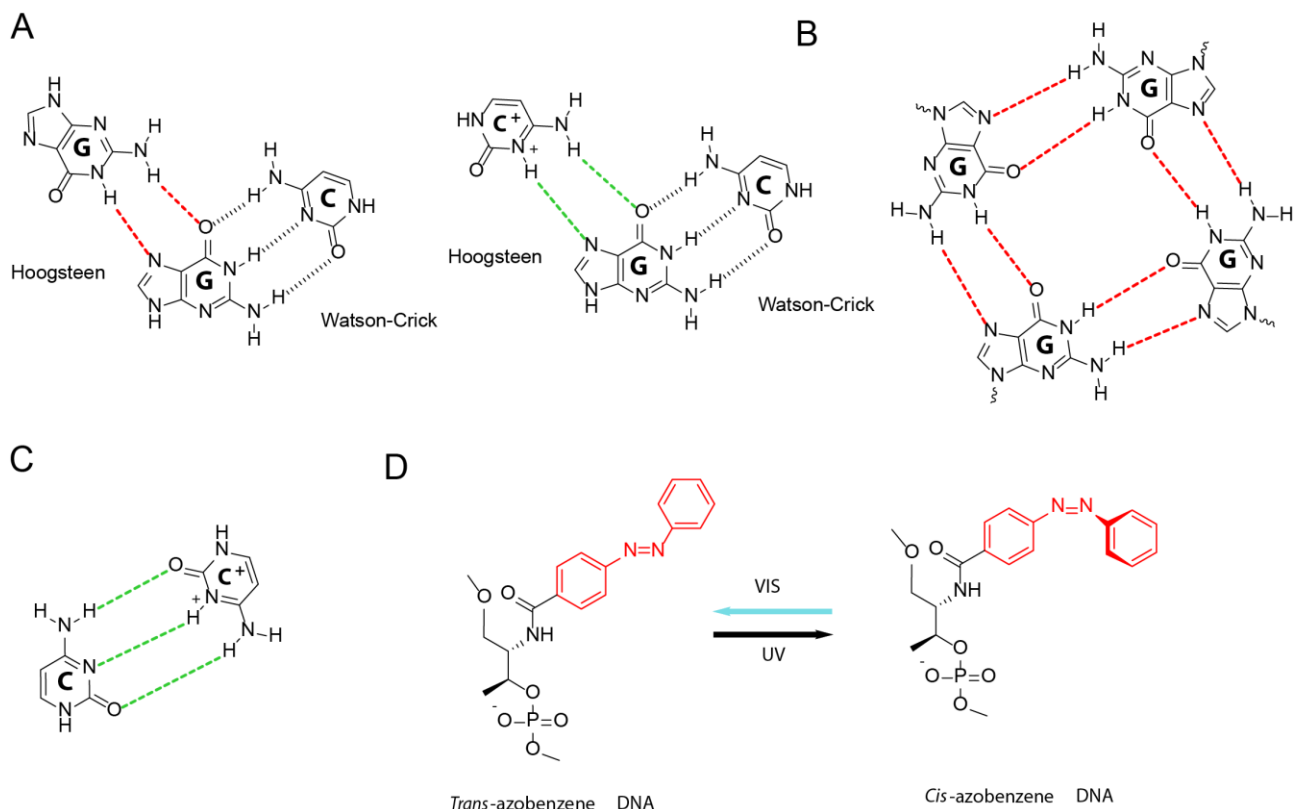


Fig. 3 DNA structures that are sensitive to pH, ionic concentration and photoactivation. **a** Non-canonical Hoogsteen hydrogen-bonding patterns for G·G and G·C⁺ (red and green), shown beside the canonical Watson-Crick hydrogen bonding pattern of G·C (black). These form the basis of G-quadruplex and DNA triplex formation respectively. **b** The G-tetrad, formed by cyclic Hoogsteen bonded square planar alignments of four guanines that are stabilized by bound monovalent Na⁺ and K⁺ cations (red). G-quadruplexes are formed by stacking of G-tetrads. **c** Semiprotonated C·C⁺ base pairs (green), which are intercalated to form the pH sensitive i-motif. **d** *trans*-*cis* photoisomerization of azobenzene modification under UV and visible light (Vis) can be used to control DNA strand hybridization (*trans*) and dissociation (*cis*).

1
2
3
4
5
6
7
8
9
10
11
12
13
14
15
16
17
18
19
20
21
22
23
24
25
26
27
28
29
30
31
32
33
34
35
36
37
38
39
40
41
42
43
44
45
46
47
48
49
50
51
52
53
54
55
56
57
58
59
60
61
62
63
64
65

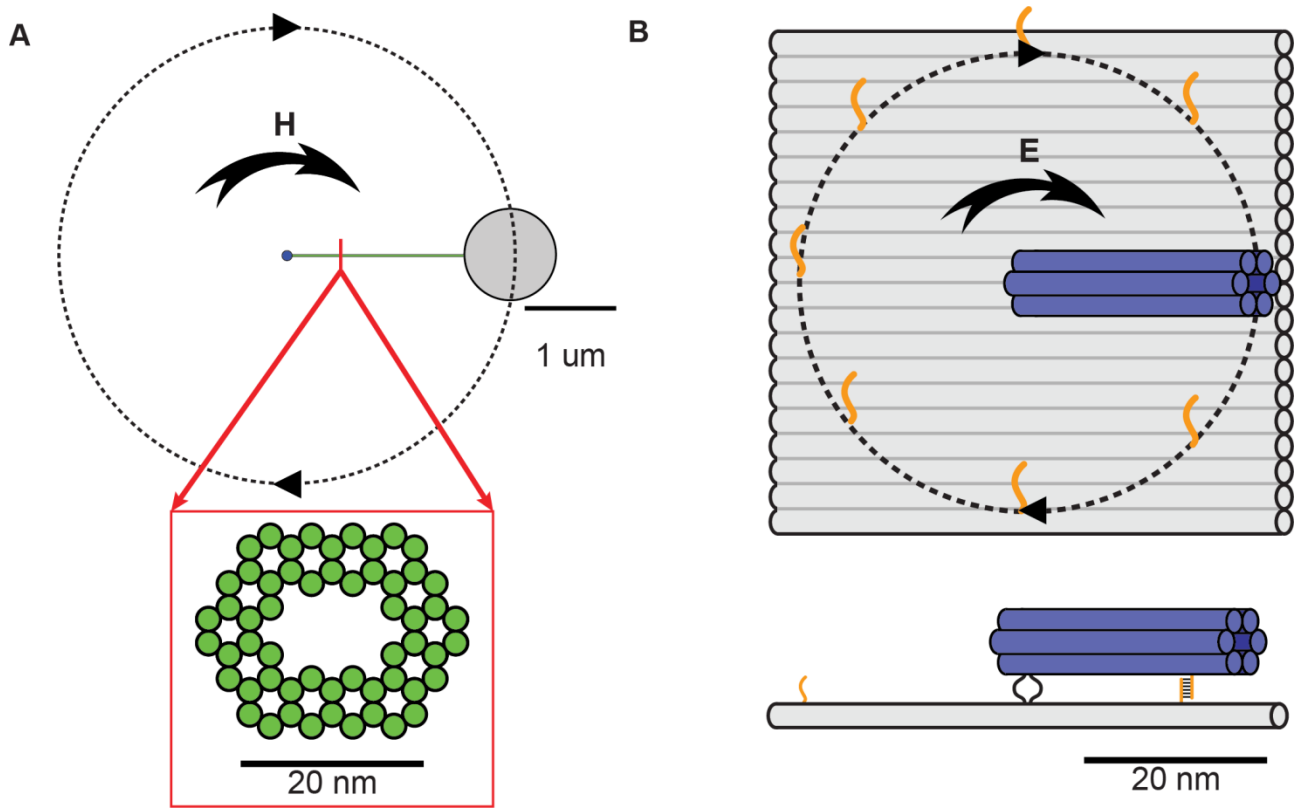


Fig. 4 Externally actuated DNA-origami nanostructures by electric and magnetic fields. **a** A DNA-origami 'lever' (green), 1-10 μm in length and with 56-helix cross-section (inset), is attached to a surface by a freely rotating linker. The other end is decorated with a 1 μm diameter magnetic nanoparticle. Rotation of the applied external magnetic field (\vec{H}) drives rotation of the nano-lever. (Lauback et al. 2018) **b** DNA-origami nanostructures are negatively charged, and respond to applied electric fields. A 25 nm 6-helix rod (blue), is linked to a 55 nm x 55 nm DNA-origami platform (grey), by a flexible single-stranded DNA linker (black). A 'latch' strand on the underside of the rod (orange), can hybridise to a number of complementary 'catch' strands on the platform (orange). The position of the rod is controlled by the direction of the applied Electric field (\vec{E}) (Kopperger et al. 2018).

References

- 1
2
3
4
5
6
7
8
9
10
11
12
13
14
15
16
17
18
19
20
21
22
23
24
25
26
27
28
29
30
31
32
33
34
35
36
37
38
39
40
41
42
43
44
45
46
47
48
49
50
51
52
53
54
55
56
57
58
59
60
61
62
63
64
65
- Alberts B (1998) The Cell as a Collection of Protein Machines: Preparing the Next Generation of Molecular Biologists. *Cell* 92:291–294 . doi: 10.1016/S0092-8674(00)80922-8
- Andersen ES, Dong M, Nielsen MM, Jahn K, Subramani R, Mamdouh W, Golas MM, Sander B, Stark H, Oliveira CLP, Pedersen JS, Birkedal V, Besenbacher F, Gothelf KV, Kjems J (2009) Self-assembly of a nanoscale DNA box with a controllable lid. *Nature* 459:73–76 . doi: 10.1038/nature07971
- Anderson RR, Parrish JA (1981) The Optics of Human Skin. *J Invest Dermatol* 77:13–19 . doi: 10.1111/1523-1747.ep12479191
- Asanuma H, Liang X, Nishioka H, Matsunaga D, Liu M, Komiyama M (2007) Synthesis of azobenzene-tethered DNA for reversible photo-regulation of DNA functions: hybridization and transcription. *Nat Protoc* 2:203–212 . doi: 10.1038/nprot.2006.465
- Bai X, Li Z, Jockusch S, Turro NJ, Ju J (2003) Photocleavage of a 2-nitrobenzyl linker bridging a fluorophore to the 5' end of DNA. *Proc Natl Acad Sci* 100:409–413 . doi: 10.1073/pnas.242729099
- Bath J, Turberfield AJ (2007) DNA nanomachines. *Nat Nanotechnol* 2:275–284 . doi: 10.1038/nnano.2007.104
- Bell NAW, Keyser UF (2016) Digitally encoded DNA nanostructures for multiplexed, single-molecule protein sensing with nanopores. *Nat Nanotechnol* 11:645–651 . doi: 10.1038/nnano.2016.50
- Burns JR, Lamarre B, Pyne ALB, Noble JE, Ryadnov MG (2018) DNA Origami Inside-Out Viruses. *ACS Synth Biol* 7:767–773 . doi: 10.1021/acssynbio.7b00278
- Chance RR, Prock A, Silbey R (2007) Molecular Fluorescence and Energy Transfer Near Interfaces. In: *Advances in Chemical Physics*. Wiley-Blackwell, pp 1–65
- Chen H, Li R, Li S, Andréasson J, Choi JH (2017) Conformational Effects of UV Light on DNA Origami. *J Am Chem Soc* 139:1380–1383 . doi: 10.1021/jacs.6b10821
- Cherry KM, Qian L (2018) Scaling up molecular pattern recognition with DNA-based winner-take-all neural networks. *Nature* 559:370–376 . doi: 10.1038/s41586-018-0289-6
- Derr ND, Goodman BS, Jungmann R, Leschziner AE, Shih WM, Reck-Peterson SL (2012) Tug-of-War in Motor Protein Ensembles Revealed with a Programmable DNA Origami Scaffold. *Science* 338:662–665 . doi: 10.1126/science.1226734
- Dietz H, Douglas SM, Shih WM (2009) Folding DNA into Twisted and Curved Nanoscale Shapes. *Science* 325:725–730 . doi: 10.1126/science.1174251
- Douglas SM, Bachelet I, Church GM (2012) A Logic-Gated Nanorobot for Targeted Transport of Molecular Payloads. *Science* 335:831–834 . doi: 10.1126/science.1214081
- Douglas SM, Dietz H, Liedl T, Högberg B, Graf F, Shih WM (2009) Self-assembly of DNA into nanoscale three-dimensional shapes. *Nature* 459:414–418 . doi: 10.1038/nature08016

- 1 Engel MC, Smith DM, Jobst MA, Sajfutdinow M, Liedl T, Romano F, Rovigatti L, Louis AA, Doye JPK
2 (2018) Force-Induced Unravelling of DNA Origami. *ACS Nano* 12:6734–6747 . doi:
3 10.1021/acsnano.8b01844
- 4 Frangioni JV (2003) In vivo near-infrared fluorescence imaging. *Curr Opin Chem Biol* 7:626–634 .
5 doi: 10.1016/j.cbpa.2003.08.007
- 6
7 Frank-Kamenetskii MD, Mirkin SM (1995) Triplex DNA Structures. *Annu Rev Biochem* 64:65–95 .
8 doi: 10.1146/annurev.bi.64.070195.000433
- 9
10 Gehring K, Leroy J-L, Guéron M (1993) A tetrameric DNA structure with protonated cytosine-
11 cytosine base pairs. *Nature* 363:561–565 . doi: 10.1038/363561a0
- 12
13
14 Gerling T, Wagenbauer KF, Neuner AM, Dietz H (2015) Dynamic DNA devices and assemblies
15 formed by shape-complementary, non–base pairing 3D components. *Science* 347:1446–
16 1452 . doi: 10.1126/science.aaa5372
- 17
18
19 Gerweck LE, Seetharaman K (1996) Cellular pH Gradient in Tumor versus Normal Tissue: Potential
20 Exploitation for the Treatment of Cancer. *Cancer Res* 56:1194–1198
- 21
22
23 Godonoga M, Lin T-Y, Oshima A, Sumitomo K, Tang MSL, Cheung Y-W, Kinghorn AB, Dirkwager
24 RM, Zhou C, Kuzuya A, Tanner JA, Heddle JG (2016) A DNA aptamer recognising a malaria
25 protein biomarker can function as part of a DNA origami assembly. *Sci Rep* 6: . doi:
26 10.1038/srep21266
- 27
28
29 Gopinath A, Miyazono E, Faraon A, Rothmund PWK (2016) Engineering and mapping nanocavity
30 emission via precision placement of DNA origami. *Nature* 535:401–405 . doi:
31 10.1038/nature18287
- 32
33
34 Gu H, Chao J, Xiao S-J, Seeman NC (2010) A proximity-based programmable DNA nanoscale
35 assembly line. *Nature* 465:202–205 . doi: 10.1038/nature09026
- 36
37
38 Hahn J, Wickham SFJ, Shih WM, Perrault SD (2014) Addressing the Instability of DNA
39 Nanostructures in Tissue Culture. *ACS Nano* 8:8765–8775 . doi: 10.1021/nn503513p
- 40
41
42 Hamaguchi N, Ellington A, Stanton M (2001) Aptamer Beacons for the Direct Detection of Proteins.
43 *Anal Biochem* 294:126–131 . doi: 10.1006/abio.2001.5169
- 44
45
46 Heckel A, Mayer G (2005) Light Regulation of Aptamer Activity: An Anti-Thrombin Aptamer with
47 Caged Thymidine Nucleobases. *J Am Chem Soc* 127:822–823 . doi: 10.1021/ja043285e
- 48
49
50 Hwang K, Wu P, Kim T, Lei L, Tian S, Wang Y, Lu Y (2014) Photocaged DNAzymes as a General
51 Method for Sensing Metal Ions in Living Cells. *Angew Chem Int Ed Engl* 53:13798–13802 .
52 doi: 10.1002/anie.201408333
- 53
54
55 Idili A, Vallée-Bélisle A, Ricci F (2014) Programmable pH-Triggered DNA Nanoswitches. *J Am Chem*
56 *Soc* 136:5836–5839 . doi: 10.1021/ja500619w
- 57
58
59 Iwaki M, Wickham SF, Ikezaki K, Yanagida T, Shih WM (2016) A programmable DNA origami
60 nanospring that reveals force-induced adjacent binding of myosin VI heads. *Nat Commun*
61 7:13715 . doi: 10.1038/ncomms13715
- 62
63
64
65

- 1 Kassem S, Lee ATL, Leigh DA, Markevicius A, Solà J (2016) Pick-up, transport and release of a
2 molecular cargo using a small-molecule robotic arm. *Nat Chem* 8:138–143 . doi:
3 10.1038/nchem.2410
- 4 Ke Y, Meyer T, Shih WM, Bellot G (2016) Regulation at a distance of biomolecular interactions
5 using a DNA origami nanoactuator. *Nat Commun* 7:10935 . doi: 10.1038/ncomms10935
6
- 7 Knudsen JB, Liu L, Bank Kodal AL, Madsen M, Li Q, Song J, Woehrstein JB, Wickham SFJ, Strauss
8 MT, Schueder F, Vinther J, Krissanaprasit A, Gudnason D, Smith AAA, Ogaki R, Zelikin AN,
9 Besenbacher F, Birkedal V, Yin P, Shih WM, Jungmann R, Dong M, Gothelf KV (2015)
10 Routing of individual polymers in designed patterns. *Nat Nanotechnol* 10:892–898 . doi:
11 10.1038/nnano.2015.190
12
- 13 Kohman RE, Cha SS, Man H-Y, Han X (2016) Light-Triggered Release of Bioactive Molecules from
14 DNA Nanostructures. *Nano Lett* 16:2781–2785 . doi: 10.1021/acs.nanolett.6b00530
15
- 16 Kopperger E, List J, Madhira S, Rothfischer F, Lamb DC, Simmel FC (2018) A self-assembled
17 nanoscale robotic arm controlled by electric fields. *Science* 359:296–301 . doi:
18 10.1126/science.aao4284
19
- 20 Kroener F, Heerwig A, Kaiser W, Mertig M, Rant U (2017) Electrical Actuation of a DNA Origami
21 Nanolever on an Electrode. *J Am Chem Soc* 139:16510–16513 . doi: 10.1021/jacs.7b10862
22
- 23 Kuzuya A, Sakai Y, Yamazaki T, Xu Y, Komiyama M (2011) Nanomechanical DNA origami “single-
24 molecule beacons” directly imaged by atomic force microscopy. *Nat Commun* 2:449 . doi:
25 10.1038/ncomms1452
26
- 27 Kuzuya A, Watanabe R, Yamanaka Y, Tamaki T, Kaino M, Ohya Y (2014) Nanomechanical DNA
28 Origami pH Sensors. *Sensors* 14:19329–19335 . doi: 10.3390/s141019329
29
- 30 Kuzyk A, Schreiber R, Fan Z, Pardatscher G, Roller E-M, Högele A, Simmel FC, Govorov AO, Liedl T
31 (2012) DNA-based self-assembly of chiral plasmonic nanostructures with tailored optical
32 response. *Nature* 483:311–314 . doi: 10.1038/nature10889
33
- 34 Kuzyk A, Schreiber R, Zhang H, Govorov AO, Liedl T, Liu N (2014) Reconfigurable 3D plasmonic
35 metamolecules. *Nat Mater* 13:862–866 . doi: 10.1038/nmat4031
36
- 37 Kuzyk A, Urban MJ, Idili A, Ricci F, Liu N (2017) Selective control of reconfigurable chiral plasmonic
38 metamolecules. *Sci Adv* 3:e1602803 . doi: 10.1126/sciadv.1602803
39
- 40 Kuzyk A, Yang Y, Duan X, Stoll S, Govorov AO, Sugiyama H, Endo M, Liu N (2016) A light-driven
41 three-dimensional plasmonic nanosystem that translates molecular motion into reversible
42 chiroptical function. *Nat Commun* 7:10591 . doi: 10.1038/ncomms10591
43
- 44 Lauback S, Mattioli KR, Marras AE, Armstrong M, Rudibaugh TP, Sooryakumar R, Castro CE (2018)
45 Real-time magnetic actuation of DNA nanodevices via modular integration with stiff micro-
46 levers. *Nat Commun* 9:1446 . doi: 10.1038/s41467-018-03601-5
47
- 48 Lee J, Huh J-H, Kim K, Lee S (2018) DNA Origami-Guided Assembly of the Roundest 60–100 nm
49 Gold Nanospheres into Plasmonic Metamolecules. *Adv Funct Mater* 28:1707309 . doi:
50 10.1002/adfm.201707309
51
52
53
54
55
56
57
58
59
60
61
62
63
64
65

- 1
2
3
4
5
6
7
8
9
10
11
12
13
14
15
16
17
18
19
20
21
22
23
24
25
26
27
28
29
30
31
32
33
34
35
36
37
38
39
40
41
42
43
44
45
46
47
48
49
50
51
52
53
54
55
56
57
58
59
60
61
62
63
64
65
- Li J, Johnson-Buck A, Yang YR, Shih WM, Yan H, Walter NG (2018a) Exploring the speed limit of toehold exchange with a cartwheeling DNA acrobat. *Nat Nanotechnol* 1 . doi: 10.1038/s41565-018-0130-2
- Li S, Jiang Q, Liu S, Zhang Y, Tian Y, Song C, Wang J, Zou Y, Anderson GJ, Han J-Y, Chang Y, Liu Y, Zhang C, Chen L, Zhou G, Nie G, Yan H, Ding B, Zhao Y (2018b) A DNA nanorobot functions as a cancer therapeutic in response to a molecular trigger *in vivo*. *Nat Biotechnol*. doi: 10.1038/nbt.4071
- Li Z, Bai X, Ruparel H, Kim S, Turro NJ, Ju J (2003) A photocleavable fluorescent nucleotide for DNA sequencing and analysis. *Proc Natl Acad Sci* 100:414–419 . doi: 10.1073/pnas.242729199
- Lilley DMJ (2000) Structures of helical junctions in nucleic acids. *Q Rev Biophys* 33:109–159
- Liu M, Jiang S, Loza O, Fahmi NE, Šulc P, Stephanopoulos N (2018a) Rapid Photoactuation of a DNA Nanostructure using an Internal Photocaged Trigger Strand. *Angew Chem Int Ed* 57:9341–9345 . doi: 10.1002/anie.201804264
- Liu Q, Deiters A (2014) Optochemical Control of Deoxyoligonucleotide Function Via a Nucleobase-Caging Approach. *Acc Chem Res* 47:45–55 . doi: 10.1021/ar400036a
- Liu T-L, Upadhyayula S, Milkie DE, Singh V, Wang K, Swinburne IA, Mosaliganti KR, Collins ZM, Hiscock TW, Shea J, Kohrman AQ, Medwig TN, Dambournet D, Forster R, Cunniff B, Ruan Y, Yashiro H, Scholpp S, Meyerowitz EM, Hockemeyer D, Drubin DG, Martin BL, Matus DQ, Koyama M, Megason SG, Kirchhausen T, Betzig E (2018b) Observing the cell in its native state: Imaging subcellular dynamics in multicellular organisms. *Science* 360:eaq1392 . doi: 10.1126/science.aaq1392
- Majikes JM, Ferraz LCC, LaBean TH (2017) pH-Driven Actuation of DNA Origami via Parallel I-Motif Sequences in Solution and on Surfaces. *Bioconjug Chem* 28:1821–1825 . doi: 10.1021/acs.bioconjchem.7b00288
- Mao C, Sun W, Shen Z, Seeman NC (1999) A nanomechanical device based on the B–Z transition of DNA. *Nature* 397:144–146 . doi: 10.1038/16437
- Marini M, Piantanida L, Musetti R, Bek A, Dong M, Besenbacher F, Lazzarino M, Firrao G (2011) A Reversible, Autonomous, Self-Assembled DNA-Origami Nanoactuator. *Nano Lett* 11:5449–5454 . doi: 10.1021/nl203217m
- Marras AE, Zhou L, Su H-J, Castro CE (2015) Programmable motion of DNA origami mechanisms. *Proc Natl Acad Sci* 112:713–718 . doi: 10.1073/pnas.1408869112
- Maune HT, Han S, Barish RD, Bockrath M, Iii WAG, Rothmund PWK, Winfree E (2010) Self-assembly of carbon nanotubes into two-dimensional geometries using DNA origami templates. *Nat Nanotechnol* 5:61–66 . doi: 10.1038/nnano.2009.311
- Menachery A, Pethig R (2005) Controlling cell destruction using dielectrophoretic forces. *IEE Proc - Nanobiotechnology* 152:145–149 . doi: 10.1049/ip-nbt:20050010
- Modi S, Nizak C, Surana S, Halder S, Krishnan Y (2013) Two DNA nanomachines map pH changes along intersecting endocytic pathways inside the same cell. *Nat Nanotechnol* 8:459–467 . doi: 10.1038/nnano.2013.92

- 1 Omabegho T, Gurel PS, Cheng CY, Kim LY, Ruijgrok PV, Das R, Alushin GM, Bryant Z (2018)
2 Controllable molecular motors engineered from myosin and RNA. *Nat Nanotechnol* 13:34–
3 40 . doi: 10.1038/s41565-017-0005-y
- 4 Ordoukhanian P, Taylor J-S (1995) Design and Synthesis of a Versatile Photocleavable DNA Building
5 Block. Application to Phototriggered Hybridization. *J Am Chem Soc* 117:9570–9571 . doi:
6 10.1021/ja00142a028
- 7
8 Patel DJ, Phan AT, Kuryavyi V (2007) Human telomere, oncogenic promoter and 5'-UTR G-
9 quadruplexes: diverse higher order DNA and RNA targets for cancer therapeutics. *Nucleic
10 Acids Res* 35:7429–7455 . doi: 10.1093/nar/gkm711
- 11
12
13 Perrault SD, Shih WM (2014) Virus-Inspired Membrane Encapsulation of DNA Nanostructures To
14 Achieve In Vivo Stability. *ACS Nano* 8:5132–5140 . doi: 10.1021/nn5011914
- 15
16
17 Ponnuswamy N, Bastings MMC, Nathwani B, Ryu JH, Chou LYT, Vinther M, Li WA, Anastassacos
18 FM, Mooney DJ, Shih WM (2017) Oligolysine-based coating protects DNA nanostructures
19 from low-salt denaturation and nuclease degradation. *Nat Commun* 8:15654 . doi:
20 10.1038/ncomms15654
- 21
22
23 Prokup A, Hemphill J, Deiters A (2012) DNA Computation: A Photochemically Controlled AND Gate.
24 *J Am Chem Soc* 134:3810–3815 . doi: 10.1021/ja210050s
- 25
26
27 Qian L, Winfree E (2011) Scaling Up Digital Circuit Computation with DNA Strand Displacement
28 Cascades. *Science* 332:1196–1201 . doi: 10.1126/science.1200520
- 29
30
31 Rajendran A, Endo M, Katsuda Y, Hidaka K, Sugiyama H (2011) Photo-Cross-Linking-Assisted
32 Thermal Stability of DNA Origami Structures and Its Application for Higher-Temperature
33 Self-Assembly. *J Am Chem Soc* 133:14488–14491 . doi: 10.1021/ja204546h
- 34
35
36 Rajendran A, Endo M, Sugiyama H (2012) Single-Molecule Analysis Using DNA Origami. *Angew
37 Chem Int Ed* 51:874–890 . doi: 10.1002/anie.201102113
- 38
39
40 Rinker S, Ke Y, Liu Y, Chhabra R, Yan H (2008) Self-assembled DNA nanostructures for distance
41 dependent multivalent ligand-protein binding. *Nat Nanotechnol* 3:418–422 . doi:
42 10.1038/nnano.2008.164
- 43
44
45 Rothmund PWK (2006) Folding DNA to create nanoscale shapes and patterns. *Nature* 440:297–
46 302 . doi: 10.1038/nature04586
- 47
48
49 Samai S, Bradley DJ, Choi TLY, Yan Y, Ginger DS (2017) Temperature-Dependent
50 Photoisomerization Quantum Yields for Azobenzene-Modified DNA. *J Phys Chem C*
51 121:6997–7004 . doi: 10.1021/acs.jpcc.6b12241
- 52
53
54 Sannohe Y, Endo M, Katsuda Y, Hidaka K, Sugiyama H (2010) Visualization of Dynamic
55 Conformational Switching of the G-Quadruplex in a DNA Nanostructure. *J Am Chem Soc*
56 132:16311–16313 . doi: 10.1021/ja1058907
- 57
58
59 Santosh M, Maiti PK (2009) Force induced DNA melting. *J Phys Condens Matter* 21:034113 . doi:
60 10.1088/0953-8984/21/3/034113
- 61
62
63
64
65

- 1 Schueder F, Lara-Gutiérrez J, Beliveau BJ, Saka SK, Sasaki HM, Woehrstein JB, Strauss MT,
2 Grabmayr H, Yin P, Jungmann R (2017) Multiplexed 3D super-resolution imaging of whole
3 cells using spinning disk confocal microscopy and DNA-PAINT. Nat Commun 8:2090 . doi:
4 10.1038/s41467-017-02028-8
- 5 Seeman NC (1982) Nucleic acid junctions and lattices. J Theor Biol 99:237–247 . doi:
6 10.1016/0022-5193(82)90002-9
- 7
8 Song J, Li Z, Wang P, Meyer T, Mao C, Ke Y (2017) Reconfiguration of DNA molecular arrays driven
9 by information relay. Science 357:eaan3377 . doi: 10.1126/science.aan3377
- 10
11 Surana S, Bhat JM, Koushika SP, Krishnan Y (2011) An autonomous DNA nanomachine maps
12 spatiotemporal pH changes in a multicellular living organism. Nat Commun 2:340 . doi:
13 10.1038/ncomms1340
- 14
15
16 Takenaka T, Endo M, Suzuki Y, Yang Y, Emura T, Hidaka K, Kato T, Miyata T, Namba K, Sugiyama H
17 (2014) Photoresponsive DNA Nanocapsule Having an Open/Close System for Capture and
18 Release of Nanomaterials. Chem – Eur J 20:14951–14954 . doi: 10.1002/chem.201404757
- 19
20
21 Thubagere AJ, Li W, Johnson RF, Chen Z, Doroudi S, Lee YL, Izatt G, Wittman S, Srinivas N, Woods
22 D, Winfree E, Qian L (2017) A cargo-sorting DNA robot. Science 357:eaan6558 . doi:
23 10.1126/science.aan6558
- 24
25
26
27 Torelli E, Marini M, Palmano S, Piantanida L, Polano C, Scarpellini A, Lazzarino M, Firrao G (2014) A
28 DNA Origami Nanorobot Controlled by Nucleic Acid Hybridization. Small 10:2918–2926 .
29 doi: 10.1002/smll.201400245
- 30
31
32 Vink AA, Roza L (2001) Biological consequences of cyclobutane pyrimidine dimers. J Photochem
33 Photobiol B 65:101–104 . doi: 10.1016/S1011-1344(01)00245-7
- 34
35
36 Wagenbauer KF, Sigl C, Dietz H (2017) Gigadalton-scale shape-programmable DNA assemblies.
37 Nature 552:78–83 . doi: 10.1038/nature24651
- 38
39
40 Wang X, Shindel MM, Wang S-W, Ragan R (2012) Elucidating Driving Forces for Liposome Rupture:
41 External Perturbations and Chemical Affinity. Langmuir 28:7417–7427 . doi:
42 10.1021/la300127m
- 43
44
45 Weissleder R (2001) A clearer vision for *in vivo* imaging. Nat Biotechnol. doi: 10.1038/86684
- 46
47
48 Weyel XMM, Fichte MAH, Heckel A (2017) A Two-Photon-Photocleavable Linker for Triggering
49 Light-Induced Strand Breaks in Oligonucleotides. ACS Chem Biol 12:2183–2190 . doi:
50 10.1021/acscchembio.7b00367
- 51
52
53 Wickham SFJ, Bath J, Katsuda Y, Endo M, Hidaka K, Sugiyama H, Turberfield AJ (2012) A DNA-based
54 molecular motor that can navigate a network of tracks. Nat Nanotechnol 7:169–173 . doi:
55 10.1038/nnano.2011.253
- 56
57
58 Willner EM, Kamada Y, Suzuki Y, Emura T, Hidaka K, Dietz H, Sugiyama H, Endo M (2017) Single-
59 Molecule Observation of the Photoregulated Conformational Dynamics of DNA Origami
60 Nanoscissors. Angew Chem Int Ed 56:15324–15328 . doi: 10.1002/anie.201708722
- 61
62
63
64
65

- 1 Xu H, Jones S, Choi B-C, Gordon R (2016) Characterization of Individual Magnetic Nanoparticles in
2 Solution by Double Nanohole Optical Tweezers. *Nano Lett* 16:2639–2643 . doi:
3 10.1021/acs.nanolett.6b00288
- 4 Yang Y, Endo M, Hidaka K, Sugiyama H (2012) Photo-Controllable DNA Origami Nanostructures
5 Assembling into Predesigned Multiorientational Patterns. *J Am Chem Soc* 134:20645–
6 20653 . doi: 10.1021/ja307785r
- 7
8 Yang Y, Hughes RP, Aprahamian I (2014) Near-Infrared Light Activated Azo-BF₂ Switches. *J Am*
9 *Chem Soc* 136:13190–13193 . doi: 10.1021/ja508125n
- 10
11 Yurke B, Turberfield AJ, Jr APM, Simmel FC, Neumann JL (2000) A DNA-fuelled molecular machine
12 made of DNA. *Nature* 406:605–608 . doi: 10.1038/35020524
- 13
14
15 Zadegan RM, Lindau EG, Klein WP, Green C, Graugnard E, Yurke B, Kuang W, Hughes WL (2017)
16 Twisting of DNA Origami from Intercalators. *Sci Rep* 7:7382 . doi: 10.1038/s41598-017-
17 07796-3
- 18
19
20 Zhang DY, Seelig G (2011) Dynamic DNA nanotechnology using strand-displacement reactions. *Nat*
21 *Chem* 3:103–113 . doi: 10.1038/nchem.957
- 22
23
24 Zhao Y-X, Shaw A, Zeng X, Benson E, Nyström AM, Högberg B (2012) DNA Origami Delivery System
25 for Cancer Therapy with Tunable Release Properties. *ACS Nano* 6:8684–8691 . doi:
26 10.1021/nn3022662
- 27
28
29 Zhou L, Marras AE, Su H-J, Castro CE (2015) Direct Design of an Energy Landscape with Bistable
30 DNA Origami Mechanisms. *Nano Lett* 15:1815–1821 . doi: 10.1021/nl5045633
- 31
32
33
34
35
36
37
38
39
40
41
42
43
44
45
46
47
48
49
50
51
52
53
54
55
56
57
58
59
60
61
62
63
64
65